

Supplementary Materials for

Key Roles for the Lipid Signaling Enzyme Phospholipase D1 in the Tumor Microenvironment During Tumor Angiogenesis and Metastasis

Qin Chen, Tsunaki Hongu, Takanobu Sato, Yi Zhang, Wahida Ali, Julie-Ann Cavallo, Adrianus van der Velden, Huasong Tian, Gilbert Di Paolo, Bernhard Nieswandt, Yasunori Kanaho, Michael A. Frohman*

*To whom correspondence should be addressed. E-mail: michael@pharm.stonybrook.edu

Published 6 November 2012, *Sci. Signal.* **5**, ra79 (2012)
DOI: 10.1126/scisignal.2003257

The PDF file includes:

- Fig. S1. Generation and characterization of PLD1-deficient mice.
- Fig. S2. Tumor growth is comparable in *Pld1*^{+/-}, *Pld2*^{-/-}, and wild-type mice.
- Fig. S3. Macrophage infiltration is comparable in wild-type and *Pld1*^{-/-} tumors.
- Fig. S4. Tumor angiogenesis is comparable in *Pld2*^{-/-} and wild-type mice.
- Fig. S5. *Pld1*^{-/-} and wild-type lung endothelial cells proliferate at comparable rates.
- Fig. S6. VEGFR2 abundance is comparable in wild-type and *Pld1*^{-/-} endothelial cells.
- Fig. S7. FIPI-treated mice do not exhibit weight loss.
- Fig. S8. JON/A inhibits activation of $\alpha_{IIb}\beta_3$ integrin and tumor metastasis.

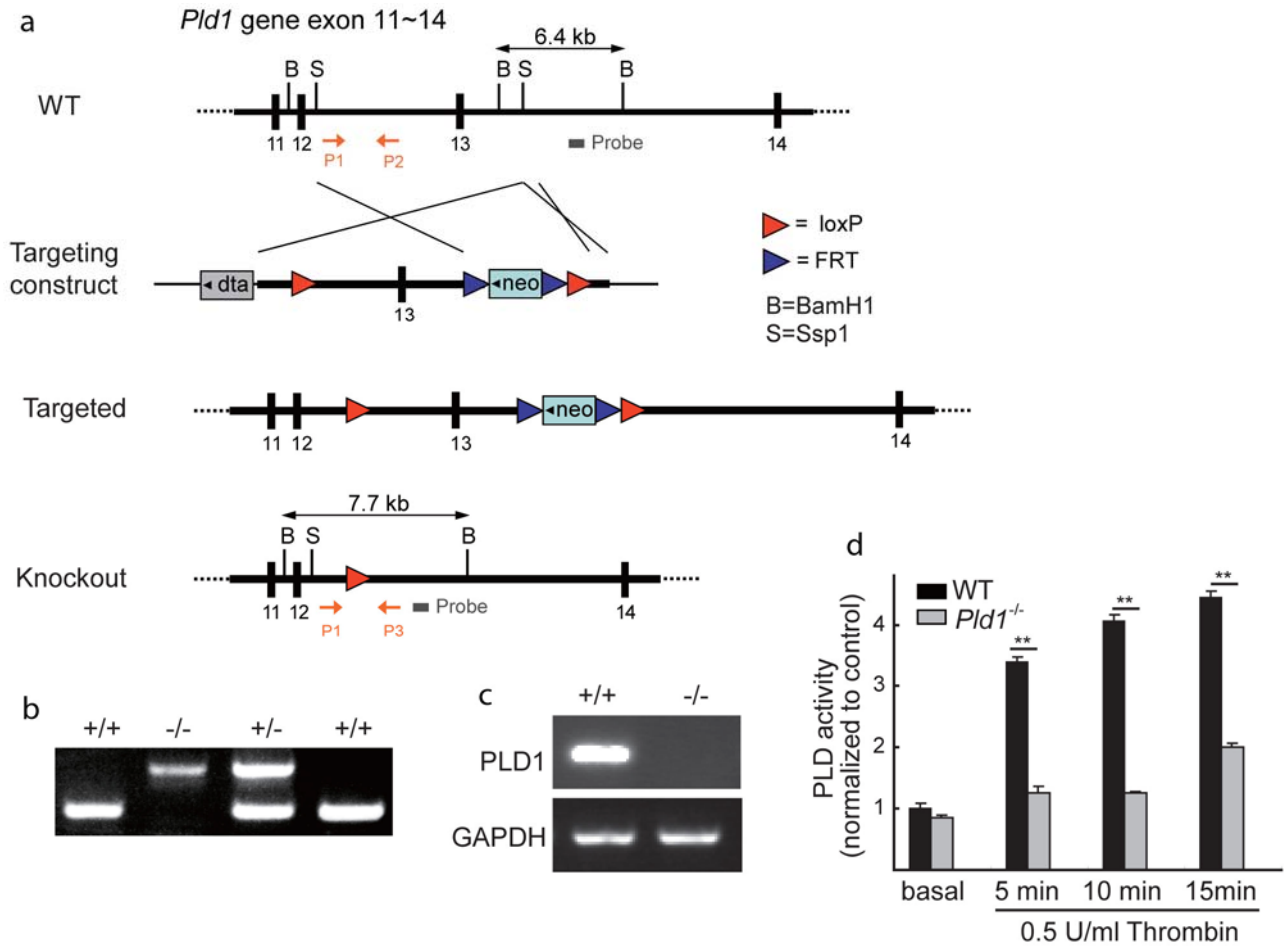


Fig. S1. Generation and characterization of PLD1-deficient mice. **A**, Targeting strategy. Shown is the genomic structure of the *Pld1* locus (wild-type, WT), a linearized *Pld1* targeting vector (Targeting construct), a targeted *Pld1* allele (Targeted) and the *Pld1* knockout allele produced by Cre recombinase-mediated deletion of a floxed exon 13 (Knockout). Neo: neomycin resistance. **B**, PCR analysis of wild-type (+/+), *Pld1*^{-/-} (-/-) and heterozygous (+/-) genomic DNA. **C**, RT-PCR analysis of PLD1 expression in wild-type and *Pld1*^{-/-} endothelial cells. **D**, PLD activities of wild-type and *Pld1*^{-/-} platelets measured under resting conditions or upon stimulation with 0.5 U/ml thrombin, average of 3 independent experiments. **, *P* < 0.01.

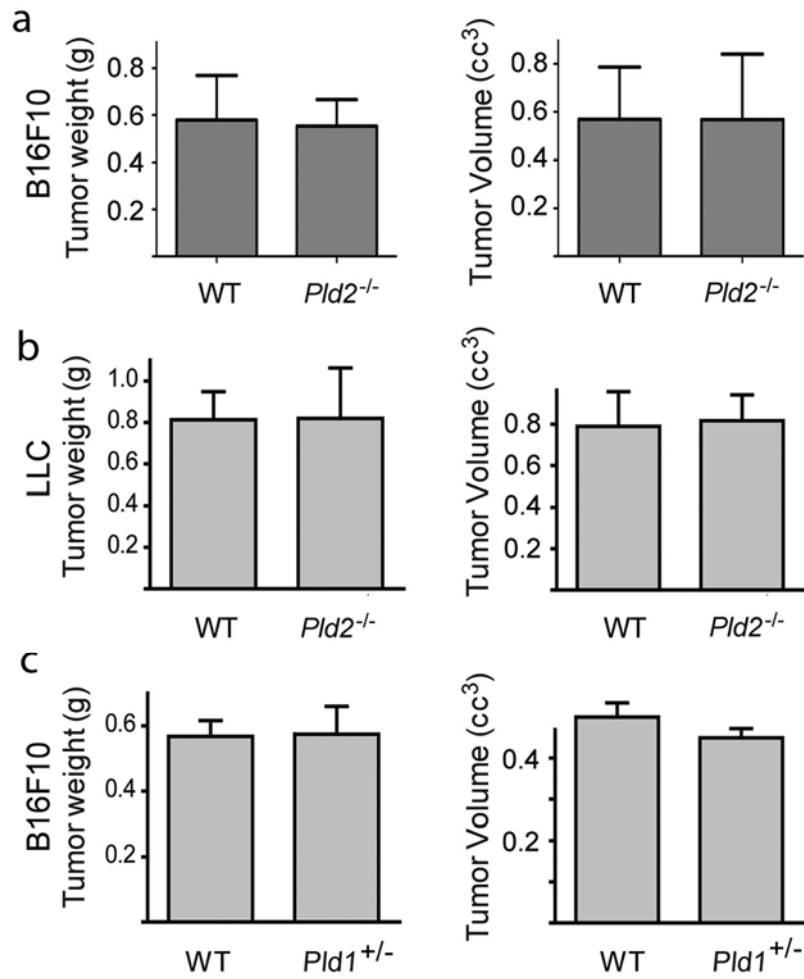


Fig. S2. Tumor growth is comparable in *Pld1*^{+/-}, *Pld2*^{-/-}, and wild-type mice. **A-C**, Mouse B16F10 melanoma (**A**, **C**) and Lewis Lung Carcinoma (**B**) tumor cells were implanted s.c. in wild-type (**A-C**), *Pld2*^{-/-} (**A**, **B**), and *Pld1*^{-/-} (**C**) mice and the resulting *in situ* tumors removed 10 days later for analysis. Tumor weights and volumes were determined as described in the legend to Fig. 1.

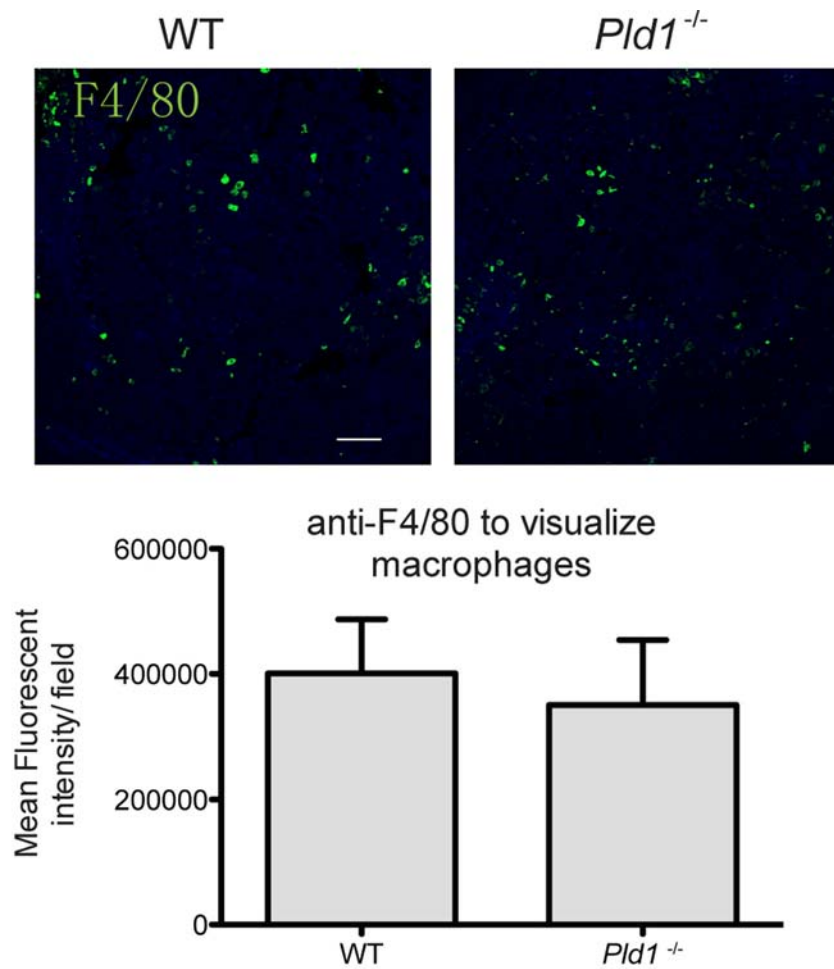


Fig. S3. Macrophage infiltration is comparable in wild-type and *Pld1*^{-/-} tumors. Macrophage infiltration was detected by immunostaining sections of B16F10 tumors implanted in wild-type and *Pld1*^{-/-} mice using a rat anti-F4/80 monoclonal antibody (Abcam). Quantitation of mean fluorescent intensity per field was performed using NIH Image J Software (n = 4 fields).

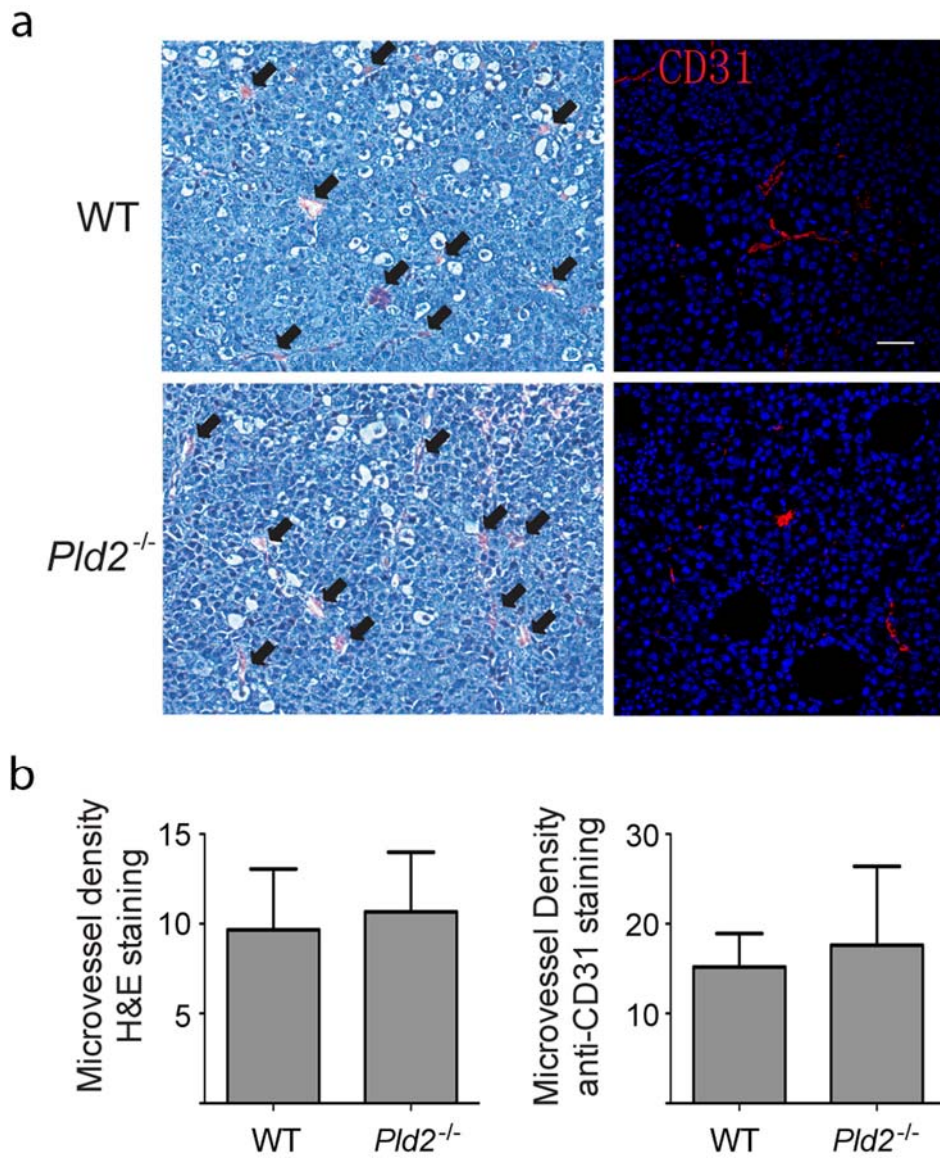


Fig. S4. Tumor angiogenesis is comparable in *Pld2*^{-/-} and wild-type mice. **A**, Sections of B16F10 tumors implanted in wild-type (upper) and *Pld2*^{-/-} (lower) mice were stained by hematoxylin and eosin (left) and anti-CD31 antibody (right). Microvessels are evident in tumors from both wild-type and *Pld2*^{-/-} mice. Scale bar: 50 μ m. **B**, Microvessel density was determined as described in the legend to Fig. 1.

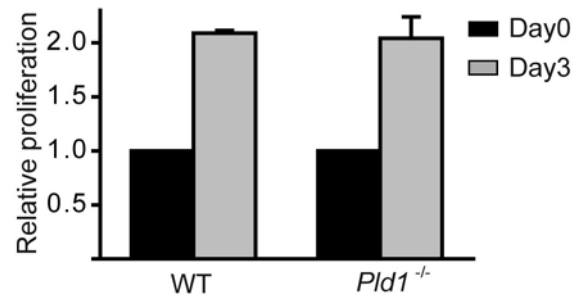


Fig. S5. *Pld1*^{-/-} and wild-type lung endothelial cells proliferate at comparable rates. a, Primary lung endothelial cells were cultured for three days. The number of viable cells was determined on days 0 and 3 using the CellTiter 96 Aqueous One solution Cell Proliferation Assay (Promega). The average of 3 experiments in triplicate is shown, normalized to the starting numbers of cells \pm s.d.

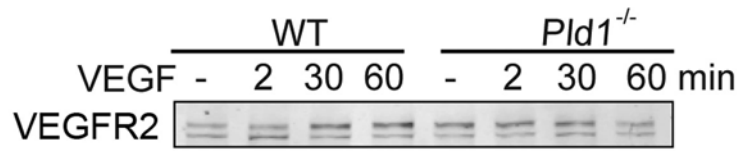


Fig. S6. VEGFR2 abundance is comparable in wild-type and *Pld1*^{-/-} endothelial cells. Endothelial cells serum-starved for 4 hours were stimulated with VEGF (50 ng/ml) for indicated times, lysed, and analyzed by Western blotting using antibodies against VEGFR2. Representative experiment of 3 shown.

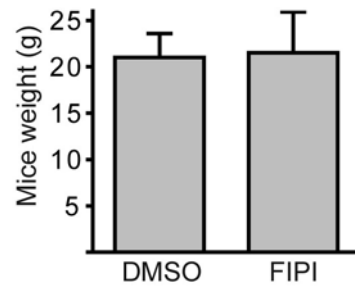


Fig. S7. FIPI-treated mice do not exhibit weight loss. Mice in control and FIPI-treated groups were weighed at the beginning (18 ± 1 g) and end of the 11 days of twice-daily FIPI treatment. $n = 6$ mice per group.

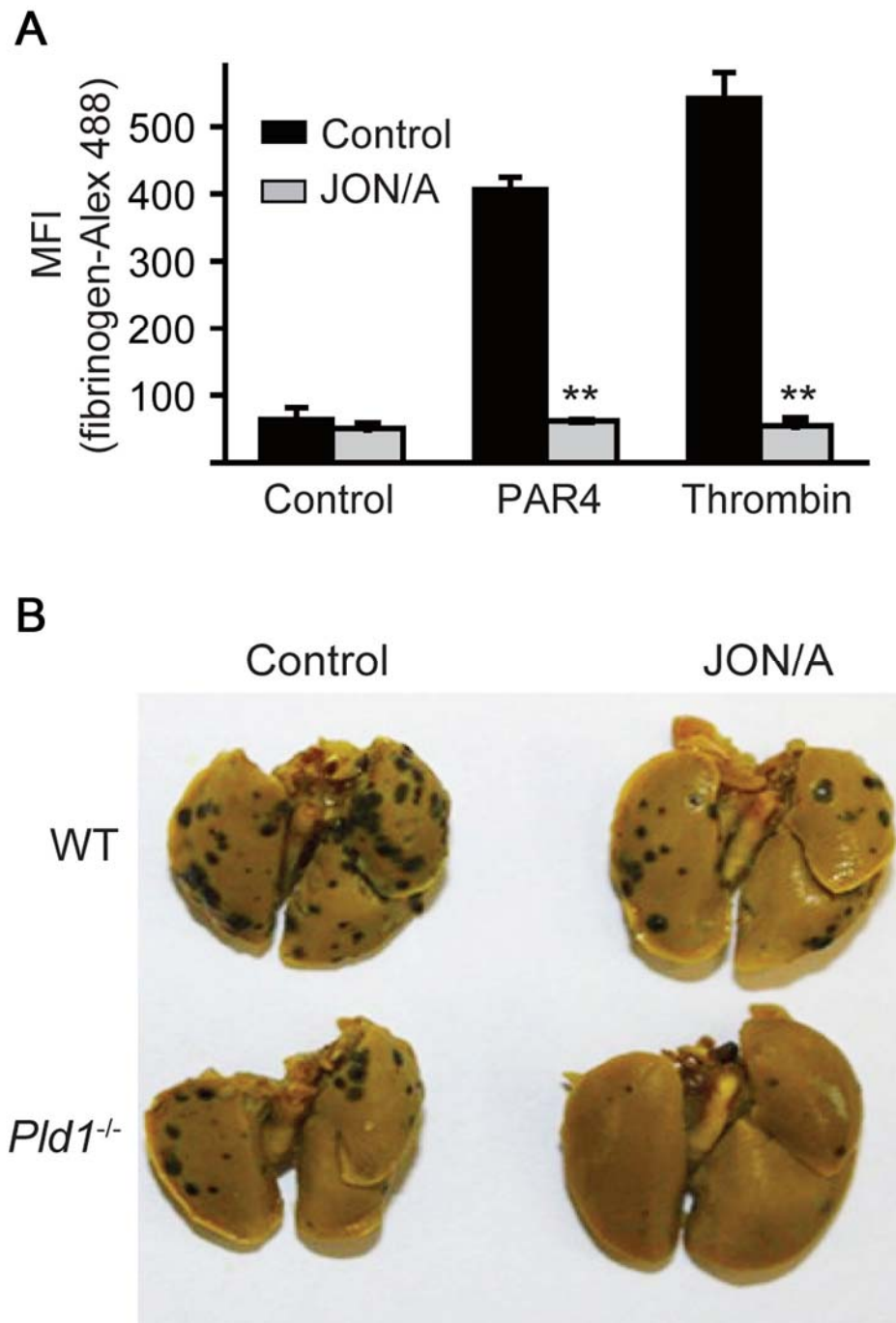


Fig. S8. JON/A inhibits activation of $\alpha_{IIb}\beta_3$ integrin and tumor metastasis. **A**, Platelets were isolated and treated with JON/A Fab fragments (5 $\mu\text{g/ml}$) or PBS for 10 min. Then platelets were then incubated with Alexa 488-labeled fibrinogen (50 $\mu\text{g/ml}$) for 10 min and stimulated with PAR4-activating peptide for 20 min or thrombin for 5 min at room temperature. Analysis was performed on a FACSCalibur (Becton Dickinson). $n=3$ independent experiments. **B**, Wild-type and *Pld1*^{-/-} mice were injected with JON/A Fab fragments (100 μg per mouse) 2 hours before injection of B16F10 cells. Lungs were removed 14 days after tumor cell injection to quantitate surface metastases ($n=12$ mice per group). Representative examples of lungs shown.